Crown breakup by Marangoni instability

By S. T. THORODDSEN[1], T. G. ETOH[2], K. TAKEHARA[2]

[1]Mechanical Engineering, National University of Singapore, 9 Engineering Drive 1, Singapore 117576
[2]Civil and Environmental Engineering, Kinki University, Higashi-Osaka 577-8502, Japan

We present experimental observations of hole formation in ejecta crowns, when a viscous drop impacts onto a thin film of low-viscosity liquid with significantly lower surface tension than the drop liquid. The holes are promoted by Marangoni-driven flows in the sheet, resulting from a spray of fine droplets ejected from the thin film hitting the inner side of the crown. The puncturing of the sheet takes place in three distinct steps. First a circular patch of the sheet thins by Marangoni-driven flows. Then this thinner film ruptures and a hole quickly opens up spanning the patch. Finally, the hole opens up further at an accelerated rate, driven by the unbalanced surface tension at its edge. The holes grow until they meet adjacent holes, thus leaving a foam-like network of liquid filaments, which then breaks up into a cloud of droplets.

1. Introduction

The impact of a drop onto a liquid surface is characterized by the formation of the well-known Edgerton crown (Worthington 1908; Edgerton & Killian 1939) which usually breaks up into droplets by capillary instability at its edge. Such edge breakup is shown, for example, for impacts onto thin liquid layers by Cossali, Coghe & Marengo (1997), Yarin & Weiss (1995) and Wang & Chen (2000), as well as in splashing due to impacts onto dry plates by Xu, Zhang & Nagel (2005). Herein, we show a qualitatively different breakup mechanism, which occurs during the impact of a viscous drop onto a liquid having lower surface tension. The splashing generates low-surface-tension droplets which impact onto the crown producing Marangoni-driven holes (Sterling & Scriven 1959). This hole-forming mechanism is similar to those used in defoaming (Garett 1993, e.g. p. 23) and in emulsification, see Danov *et al.* (1988) and references therein.

2. Experimental setup

2.1. *Impact conditions*

This study looks at the impact of a viscous water/glycerin drop onto a thin film of ethanol. Experiments were conducted for one impact velocity, but a range of drop viscosities. The impact height of the drop was kept at 4.37 m, giving an impact velocity of $7.7\,\text{m s}^{-1}$. Glycerin/water mixtures 83 % to 99 % by weight, were used to produce drops with a range of relatively large dynamic viscosities μ, from 44 to 510 cP.

The drops were generated by a gravity-driven pinch-off from a stainless steel tube with an outer diameter of 4.9 mm. The resulting drops had a horizontal diameter at impact of 5.0 mm. The drop cuts a laser beam 15 cm below the nozzle and then falls through a 4 m long pipe, to minimize sideways drift of the drop during the free-fall. The substrate was a glass plate $19 \times 19\,\text{cm}^2$ in area and 19 mm thick.

2.2. *The thin film*

The thin liquid film on the substrate was generated by allowing a small amount of ethanol (99.5 % pure) to spread on the glass plate, which it wets. The procedure used to generate reasonably repeatable film thicknesses was the following. After each impact the remnant of the glycerin/water drop was wiped off the plate with a lint-free paper towel. A small amount of water was then squirted onto the plate and wiped off to clean most of the remaining liquids. Then 0.2 ml of ethanol was fed onto the plate using a small syringe. This ethanol would often spread unevenly due to minute, but unavoidable liquid remnants from the previous impact. This ethanol was then wiped off, leaving a very thin residual ethanol film spread fairly evenly over the impact region. Then another 0.2 ml of ethanol was fed onto the plate, which now spread evenly away from the centre, generating a symmetric film. It was allowed to spread for about 40 s, which generated a wetting spot of around 7 cm in diameter, before the next impact. With no evaporation and even spreading, the film would be $\delta \simeq 50\,\mu\mathrm{m}$ thick, as an upper bound. The evaporation rate of the ethanol was estimated using a sensitive balance, under the same conditions as the experiments, with air temperature around 30 °C. This gave a refined estimate of $\delta \simeq 35\,\mu\mathrm{m}$.

2.3. *Range of parameters*

The Weber and Reynolds numbers are calculated based on the horizontal diameter of the drop D and the impact velocity U. The film thickness δ is not the relevant length scale in the current configuration, as the splashing sheet leaves the free surface and does not flow within the film. The liquid properties can however be based on the viscosity and surface tension either of the drop liquid ν_d and σ_d, or of the thin film ν_f and σ_f. Based on the film properties these numbers are kept fixed:

$$We_f = \rho_f DU^2/\sigma_f = 10500, \quad Re_f = DU/\nu_f = 39000.$$

The same numbers using the drop properties, over the range of drop viscosities, give

$$We_d = \rho_d DU^2/\sigma_d \simeq 5600, \quad Re_d = DU/\nu_d = 95 - 1100,$$

where $\sigma = 65$ for the glycerin/water mixture and $\sigma = 22$ dyn cm^{-1} for the ethanol.

2.4. *Ultra-high-speed video camera*

Detailed observations of the breakup process were accomplished with an ultra-high-speed video camera developed by Etoh *et al.* (2003), using frame rates up to 200 000 frames s^{-1}. The prototype (Shimadzu Corp.) acquires 103 frames, of 260×312 pixels each, irrespective of the frame rate. Backlighting was used to form a silhouette of the phenomenon.

Some still images with much higher spatial resolution, were also taken using a digital camera (Nikon D100, 3008×2000 px) and xenon flash-lamps with flash duration of 2 μs.

3. Results

Figure 1 shows a typical example of the crown-breakup mechanism. During the initial contact it shows the violent horizontal splashing of the ethanol film into what appears to be a spray of fine droplets. The initial horizontal speed of this splash is estimated, from the first three frames, to be about 100 m s^{-1}, consistent with the experiments of Thoroddsen (2002). This is followed by a continuous sheet of ethanol, which is now ejected more in the vertical direction at the edge of the drop. Subsequently, 250 μs after first contact, the drop liquid starts to form a bowl (light
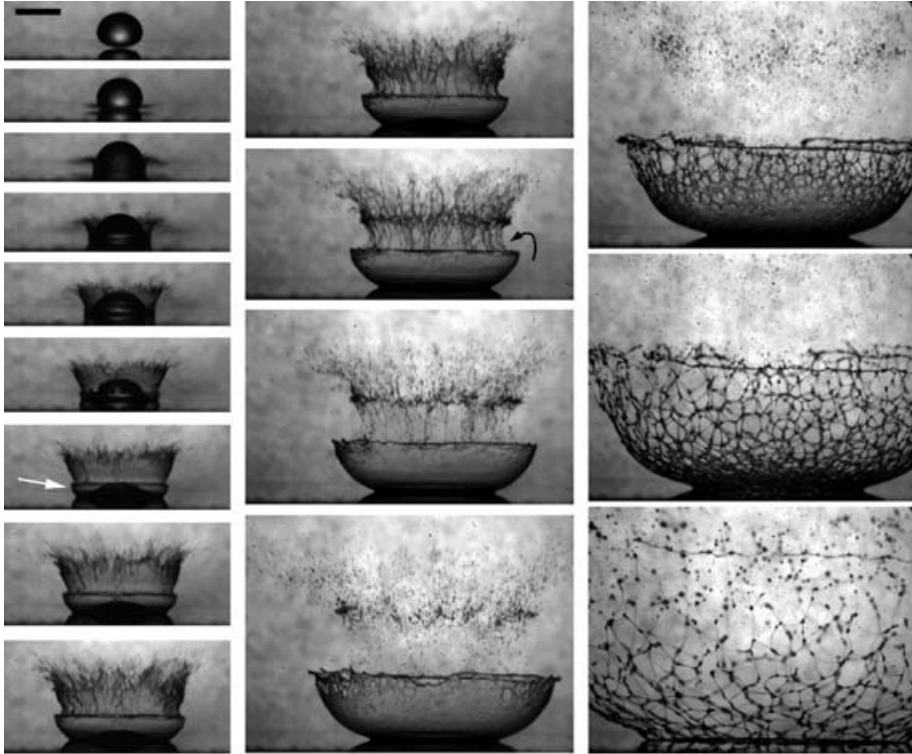
FIGURE 1. The impact of a viscous drop onto a 35 µm film of ethanol. Drop is 89 % glycerin, giving $Re_d = 460$ and $We_d = 5720$. Times shown are 0, 50, 100, 150, 200, 250, 350, 450, 550, 650, 800, 1050, 1400, 2000, 2800 and 4600 µs after first contact. The scale bar is 5 mm long. See also the movie available with the online version of the paper.

arrow in panel 7), which emerges out of the bottom film and follows the ethanol sheet. These two parts are connected, forming a continuous liquid sheet. The dynamics of the two parts are quite different, however, with the viscous drop liquid forming an ever larger bowl, whereas the very thin ethanol sheet starts to be pulled back towards the axis of symmetry, owing to two effects. First, the surface tension pulls it inwards, up to the time when it buckles and breaks up into vertical striations, as is evident in the 11th panel of figure 1. Secondly, the air flow around the crown (dark arrow) will force this pull-back of the ethanol sheet. The inertia of the viscous sheet, forming the bowl, is much larger than that of the ethanol sheet, because it is much thicker. It is therefore not pulled back as much by its own surface tension. The expanding crown must pull in air over its sides, or from the top. The edge of the crown can be thought of as a flat plate moving in quiescent air. In the reference frame moving with this edge the air is driven around the corner, as indicated by the arrows in figures 1 and 4(*d*). If we assume irrotational motions in the air, the deflection of the ethanol sheet should be largest closest to the edge, just as is observed. The boundary layer in the air along the outer edge of the crown, might also separate forming a vortex, with similar effect.

The origins of the liquid in the two parts of the sheet are verified in figure 2, where we have mixed Fluorescein dye $(0.2 \, \mathrm{g} \, \mathrm{l}^{-1})$ into the drop liquid and taken a still colour image. The bluish reflections from the top part of the sheet confirm this liquid is from the thin ethanol film, as it shows none of the fluorescent light arising from the drop liquid.

The ethanol sheet continues to shed droplets from its fraying upper edge, resembling a flower arrangement, before breaking up into a cloud of droplets, which rises
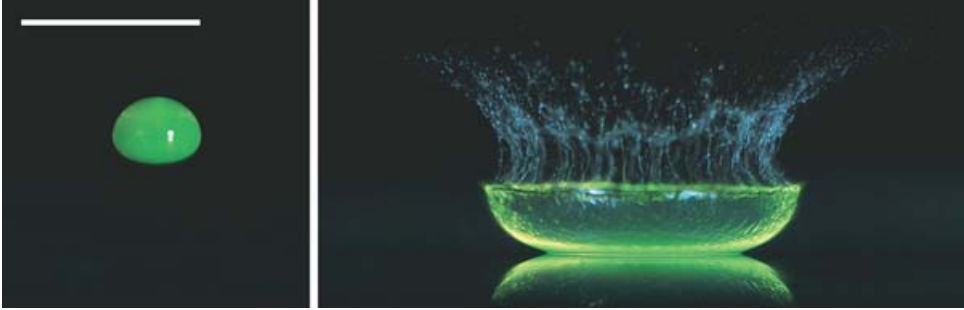
FIGURE 2. The impact of a drop containing Fluorescein dye, for similar impact conditions as in figure 1. The scale bar is 10 mm long.

upwards away from the crown. The ethanol closest to the contact point with the crown also breaks apart, as shown in the sequence in figure 1 and in closeup photos in figure 4(*c, d*). This figure also shows that the breakup forms vertical striations of liquid, which are about 5 μm thick. This suggests that the ethanol sheet is sub-micron thick and can break up by random velocity fluctuations. The resulting ethanol droplets close to the bowl are now flung downwards by the air flow, towards the inside surface of the bowl, where they start to puncture holes in the crown.

3.1. *The hole formation*

We observe that the puncturing of the sheet takes place in three distinct steps, as shown in the close-up images and sketch in figure 3. Following the contact of the spray droplet, a circular patch of the sheet thins by Marangoni-driven flows, where the lower-surface-tension drop liquid is pulled apart by the crown liquid. Then this thinner film ruptures (arrow in figure 3*a*) and quickly opens up a hole spanning the patch. Finally, the hole grows at an accelerated rate, driven by the unbalanced surface tension at its edge. The holes grow until they meet adjacent holes, thus leaving a net-like structure of liquid filaments, see figure 4(*f*). As there are no surfactants to stabilize the interfaces, this is a fleeting construct which quickly breaks up into a cloud of droplets.

The growth rate of the Marangoni patches can be measured from the video. The patch highlighted in figure 3(*b*) was tracked before the rupture. From 160 to 80 μs before the rupture its radius expands at 0.6 m s^{-1}, whereas during the last 80 μs before the rupture it has accelerated slightly to 0.8 m s^{-1}. The apparent acceleration is not surprising, as the viscous forces, counteracting the Marangoni stress at the surface, can be expected to scale with the thickness of the liquid film, which is rapidly thinning just before the rupture. Other patches show similar radial velocities just before rupture, between 0.57 and 0.85 m s^{-1}. These velocities are reasonably consistent with measurements of Marangoni-driven spreading on deep pools (Dussaud & Troian 1998; Ruckenstein, Smigelschi & Suciu 1970 and Santiago-Rosanne, Vignes-Adler & Velarde 1997) and theory reviewed by Jensen (1995).

The speed of the rupture of the film covering the patches could be measured for a handful of cases, such as the one in figure 3(*b*). The actual rupture usually occurs at a point along the edge of the patch. The thin film contracts at speeds in the range from 12 to 22 m s^{-1}. This speed is controlled by the thickness of the film which covers the patch at the time of rupture, which will differ from one patch to another.

The speed of the edge of a growing hole was also measured for numerous holes, selected to be isolated to minimize influence from adjacent holes. These measurements gave speeds in the range 1.7 to 2.3 m s^{-1}.
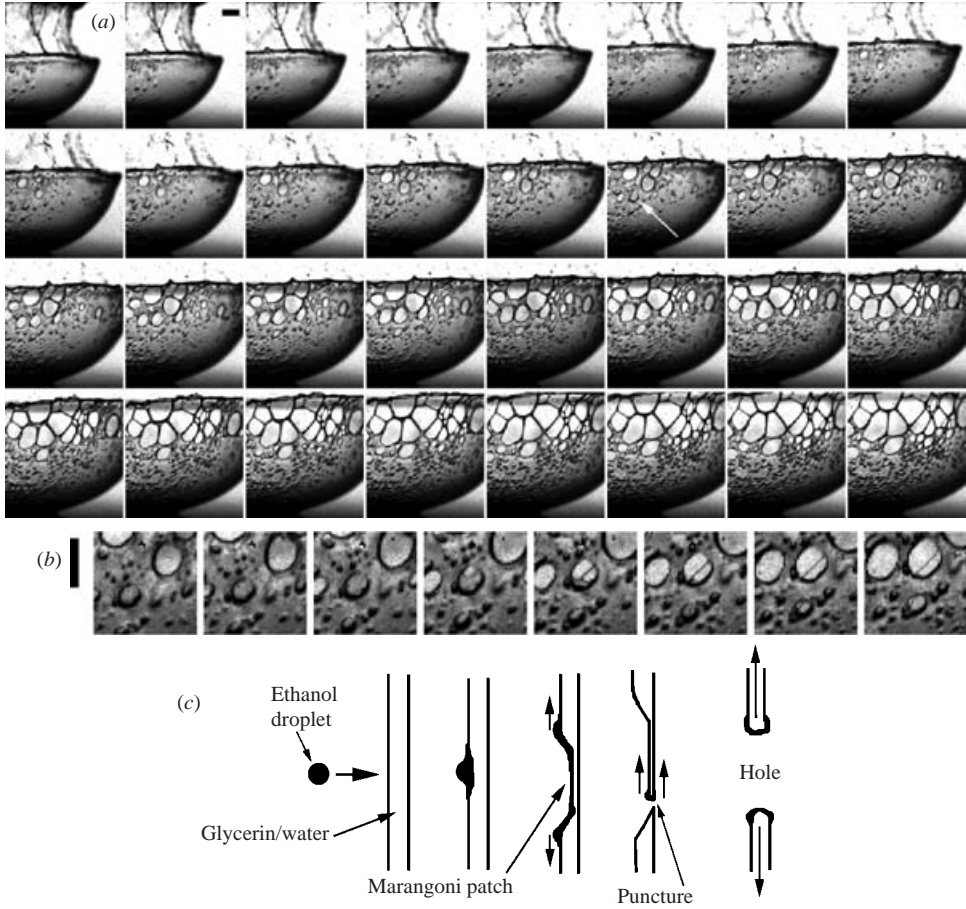
FIGURE 3. The formation of holes in the crown. (*a*) The arrow in frame 14 points to a Marangoni patch, where the thin film is in the process of puncturing. The frames are spaced by 20 μs, going from left to right and then top to bottom, spanning a total of 620 μs. (*b*) Close-up of the rupture of the patch identified in (*a*). One can also see another patch rupture directly below it. The scale bars are 1 mm. (*c*) Sketch of the three stages in the formation and growth of holes.

The retraction speed of an edge of a liquid film is a well-known problem, considered by Taylor (1959) and Culick (1960). For a liquid sheet of thickness h their model predicts that the hole will open up at a radial speed of

$$V_r = \sqrt{2\sigma/\rho h} \Rightarrow h = 2\sigma/(\rho V_r^2).$$

This gives an indirect method to estimate the film thickness. For the thin film covering the patches we find $h \simeq 0.35\,\mu\text{m}$. The thickness of the crown itself is estimated as $h \simeq 22\,\mu\text{m}$. In these estimates we have used the average surface tension of the ethanol and the glycerin/water mixture in the drop, i.e. $\sigma_{ave} = 0.044\,\text{N m}^{-1}$. Here, we assume that viscous stresses in the expanding crown do not contribute to the expansion of the hole.

We note that the Ohnesorge number $Oh = \mu/\sqrt{\rho h \sigma}$ for the opening holes takes a value $Oh \simeq 2$, using the drop viscosity. Numerical simulations by Song & Tryggvason (1999), of a two-fluid system, suggest that viscosity might therefore be slowing down the motions. Our estimates for the thickness of the crown are thus quite approximate, but overall are consistent with other estimates, as shown below.
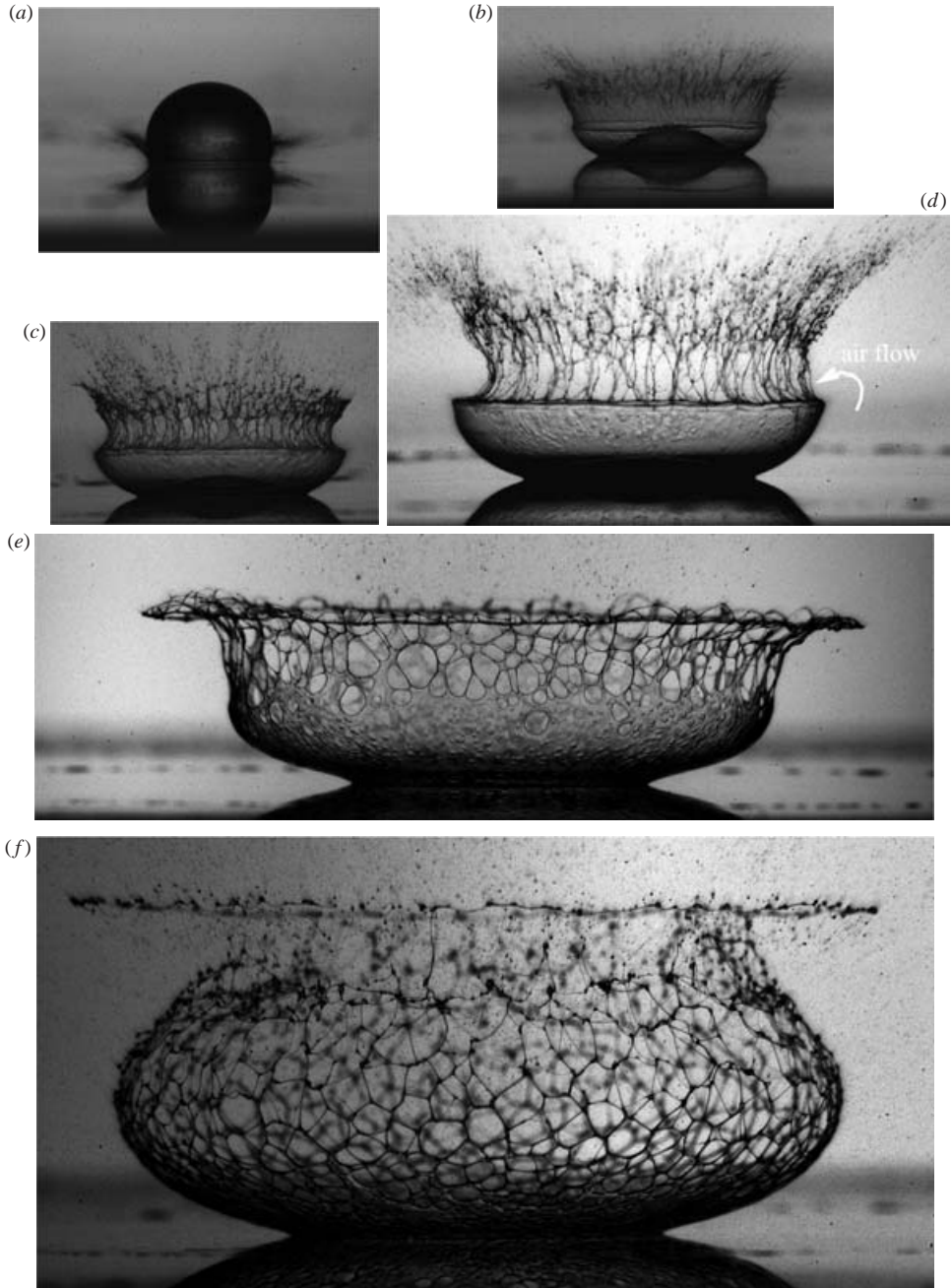
FIGURE 4. Still images taken during the impact of different drops, under similar conditions as in figure 1. (*a*) Initial splashing. (*b*) Continuous ethanol sheet. Note the bubble under the drop. (*c*) Breakup of ethanol sheet. (*d*) Ethanol sheet breaks up into filaments. (*e*) Formation of holes. Notice the thicker edge. (*f*) Network of liquid filaments. Images are not to the same scale.

The very large edge velocity of the thin film, across the patches, is around 35 times higher than the viscous velocity $V_\mu = \sigma/\mu \simeq 0.5\,\mathrm{m\,s^{-1}}$. This suggests that the mixing of the ethanol with the crown liquid must have significantly reduced the viscosity of these thin films, as $Oh \simeq 20$ in this case, based on the crown viscosity.

Figure 4 shows higher-resolution still images of some stages of the breakup process.
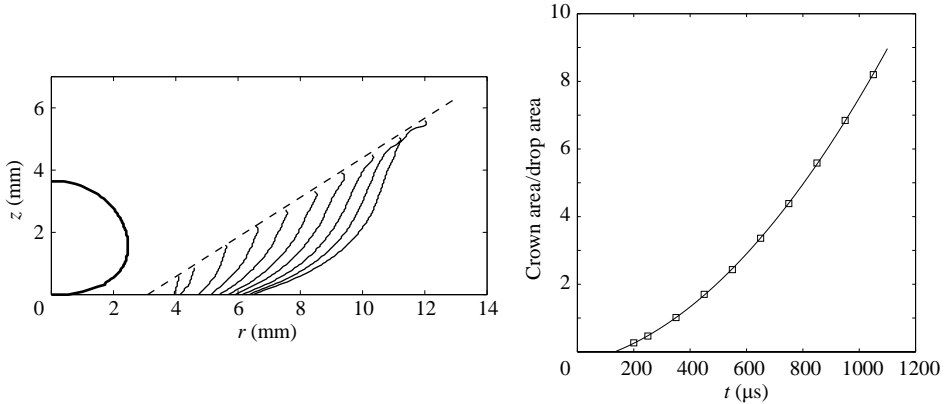
FIGURE 5. (*a*) The crown shapes are shown at 200, 250 and thereafter at intervals of 100 μs after first contact of the drop. The crown height vs. its radius r is approximated by $z = 0.62\,(r - R)$, where R is the drop radius. The drop shape at first contact is also shown. (*b*) The crown area vs. time. The area is normalized by the original drop area.

3.2. *Crown shape and thickness*

In figure 5 we have traced the crown shape during the early growth, before breakup. The area of the crown grows to about 8 times the original drop area during the first 1 ms. The growth follows a parabolic curve. We note that a large remnant of the viscous drop, remains on the plate at the centre after the impact. If we assume that half of the drop liquid enters the crown, then the average thickness of the sheet in the last curve of figure 5(*a*) is $\bar{h} \simeq 45\,\mu\text{m}$ at 1050 μs after the first contact. We propose that the initial sheet is thinnest (Thoroddsen 2002) and in combination with the stretching caused by the axisymmetry, we estimate the sheet thickness as between 10–70 μm, which encompasses the previous estimate.

Taking both surfaces of the crown into account, along with the central region, the surface energy σA has grown by a factor of about 20 in the first 1 ms. However, the ratio of kinetic to surface energies for $We = 5600$ is

$$\frac{E_{kin}}{E_{surf}} = \frac{\frac{1}{2}\left(\rho\frac{4}{3}\pi R^3\right)U^2}{\sigma\,4\pi R^2} = \frac{\rho(2R)U^2}{12\sigma} = \frac{We}{12} \sim 500.$$

We conclude that only 4 % of the kinetic energy has been converted into surface energy. The potential energy of the crown is also small. Therefore, most of the kinetic energy has either gone into propelling the splashing droplets, or been dissipated by viscous stresses.

The location and motion of the Marangoni patches allows us to determine the stretching of the fluid elements along the sheet, as the crown rises and expands. By assuming a uniform velocity throughout the thickness of the sheet, we find, for the second to last curve in figure 5(*a*), that the velocity along the sheet increases approximately linearly from the plate to the edge, giving $\partial u/\partial s = 1200\,\text{s}^{-1}$. The tangential stress in a plane through the axis of symmetry $\mu(\partial u/\partial s)$ is therefore of comparable strength to the azimuthal stress produced by the strain rate due to the axisymmetry $\mu(u_r/r)$, which at the centre of this curve is $u_r/r \simeq 470\,\text{s}^{-1}$.

3.3. *Impact on a dry plate*

For comparison, figure 6 shows the impact of the same drop onto a dry glass plate. No splashing is observed, demonstrating how strongly the viscous stresses due to the no-slip boundary condition can arrest the lamella travelling along the glass plate.
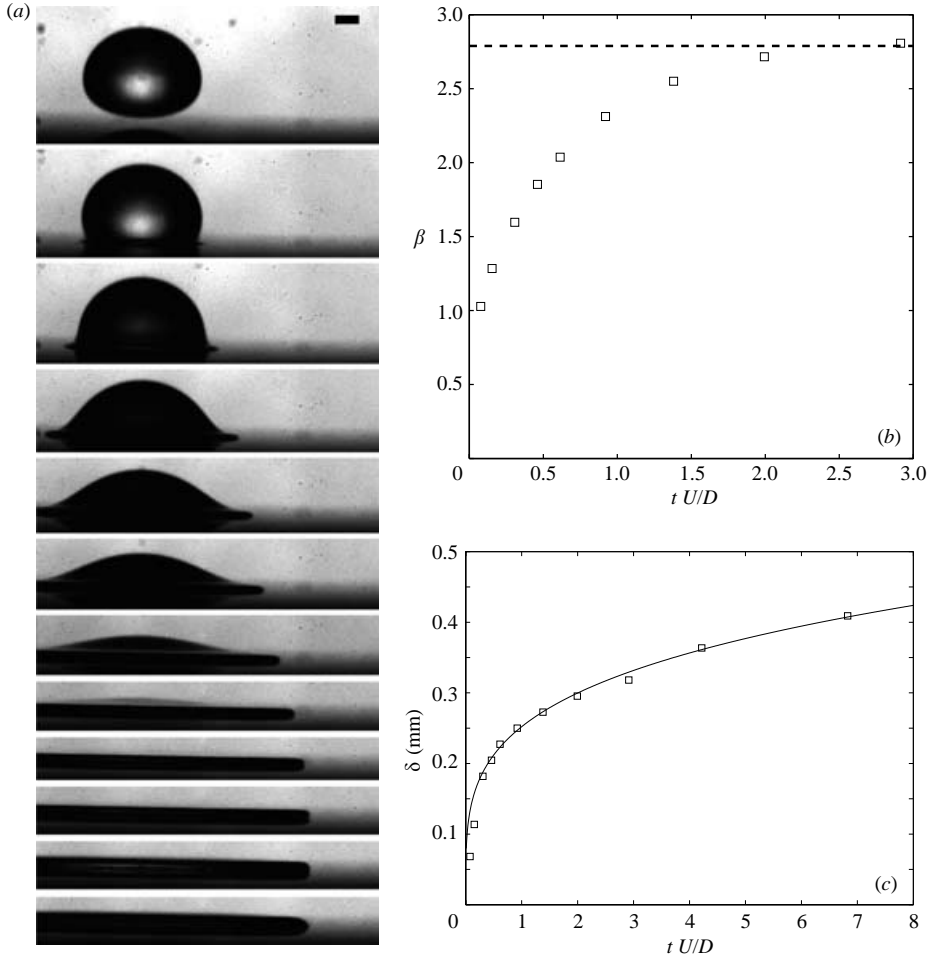
FIGURE 6. The impact of a viscous drop onto a dry glass plate, $Re_d = 460$ and $We_d = 5720$. (*a*) The evolution of the impact lamella travelling along the plate. The times shown are −50, 50, 100, 200, 300, 400, 600, 900, 1300, 1900, 2750 and 4450 µs after first contact. The scale bar is 1 mm long. (*b*) The spread-factor β vs. the normalized time. (*c*) The thickness of the lamella travelling along the plate. The solid curve shows the power law $\delta \sim (tU/D)^{0.25}$.

The spreading factor $\beta = D_{max}/D$ is 2.78 and is reached after about 1.7 ms. The shear rate in the film can be estimated, for example at $t = 150$ µs, as $U_j/\delta \simeq 55\,000\,\mathrm{s}^{-1}$, which is much larger than the above evaluations of the strain rates within the crown.

3.4. *Effects of drop viscosity*

Figure 7 shows the influence of changing the drop viscosity on the breakup mechanism. Figure 7(*a*) reveals a very similar evolution for an 88 % increase in drop viscosity using 94 % glycerin concentration. The ethanol sheet appears more 'wispy' and it has already broken into vertical stripes at 450 µs compared to 1050 µs for the case in figure 1. The bowl, on the other hand, takes longer to fully break up into a net. The puncturing takes place in two waves, first in the top layer, followed by the bowl.

For the lower drop viscosity, figure 7(*b*), the sheet breaks up earlier, without any clear demarcation line between the two liquid sheets, with the holes primarily propagating from the edge. For the largest viscosity, figure 7(*c*), the bowl is flatter and breaks up much later through the formation of large holes. The characteristic
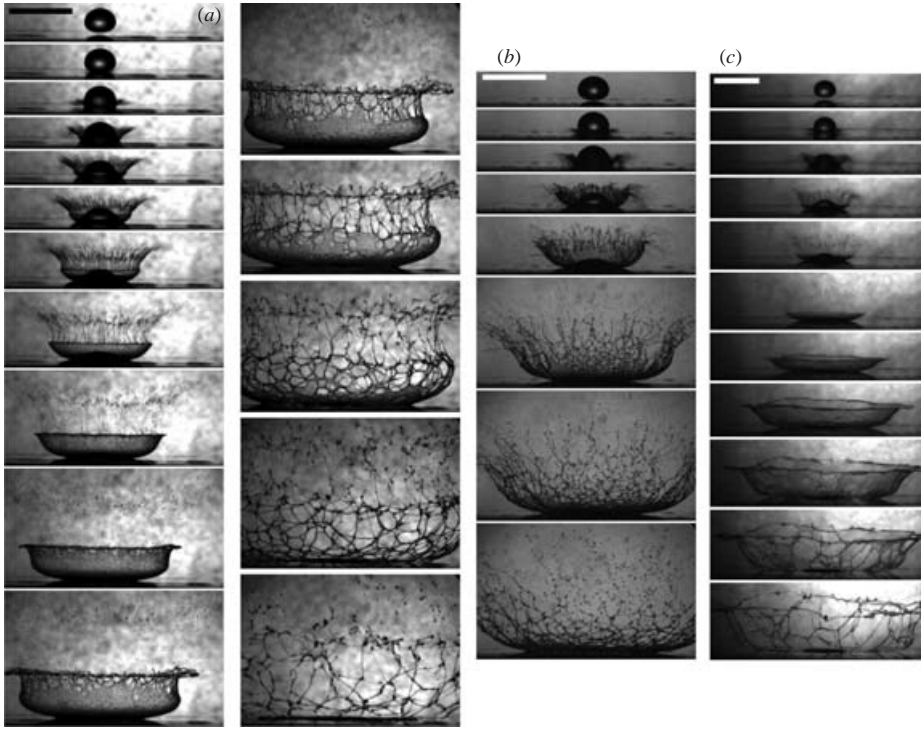
FIGURE 7. The impact of different viscosity drops. (*a*) Drop is 94 % glycerin, $Re_d = 250$ and $We_d = 5780$. Times shown are -50, 0, 50, 100, 150, 200, 300, 450, 650, 900, 1200, 1550, 2000, 2550, 3300 and 4750 μs after first contact. (*b*) The impact of a lower viscosity drop (83 % glycerin), $Re_d = 1100$ and $We_d = 5600$. Times shown are -20, 40, 100, 400, 900, 1280 and 1840 μs after first contact. (*c*) Higher viscosity drop, (99 % glycerin), $Re_d = 95$ and $We_d = 5600$. Times shown are -50, 50, 150, 250, 350, 600, 1200, 2000, 2700, 3100 and 4000 μs. All bars 10 mm.

pock-marks are no longer visible in the sheet. It is not clear whether the increased thickness of the sheet, or the trajectories of the spray droplets, have caused this reduction in the number of holes.

4. Discussion and conclusions

The apparent uniformity of holes in figure 4(*f*) is not produced by an even distribution of the spray droplets hitting the crown. Only a fraction of the seeds end up puncturing a hole (see the movie available with the online version of the paper). Once the growth of the adjacent holes creates compression in the sheet, the Marangoni patches contract and fail to puncture the thin film, becoming part of the filaments. The average separation of the holes therefore depends on the viscosity of the sheet, by determining crown thickness, as well as influencing how quickly an ethanol droplet will cause accelerated thinning. These factors affect the probability of puncture, which in turn determines hole spacing and eventual hole size. Comparison between figures 1 and 7 shows that higher drop viscosity increases the spacing of the holes.

One might envision an alternative cause for the patches in the sheet, i.e. that they are generated by a Marangoni instability at the outer contact, where the crown meets the surface film. However, this should leave an even distribution of Marangoni patches, which is not observed. Furthermore, the patches are sometimes observed to appear after the rise of the crown, as is demonstrated in the sequence of frames in figure 8. This supports our claim that the splash droplets cause the puncturing.
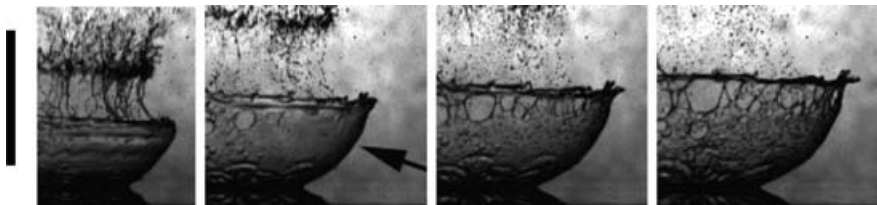
FIGURE 8. The appearance of Marangoni patches in the crown. The arrow points to a region of the crown which is free of pock-marks. Subsequent frames show the appearance of numerous patches, which we interpret as the impact of ethanol droplets, which are projected downwards from the broken ethanol sheet. The frames are taken at 1.1, 1.5, 1.7 and 1.9 ms from first contact. The scale bar is 10 mm long.

Ejecta sheets observed during the impact of a drop onto a pool of the same liquid, e.g. Thoroddsen (2002), do not break up by hole formation. We therefore rule out Rayleigh–Taylor instability, which is observed to generate holes by Bremond & Villermaux (2005) for shock-accelerated soap films. We believe the extensional viscous stress will, in our axisymmetric case, counteract this instability.

Cursory experiments with other low-σ liquids in the film, such as acetone and butanol, show similar breakup by hole formation, demonstrating that this is a generic phenomenon, which is not limited to ethanol. It may therefore find applications in numerous scientific and industrial processess. More controlled experiments, such as shooting an ethanol droplet at a falling viscous film, would be warranted. It would also be interesting to invert the surface tensions of the two liquids.

In conclusion, we have identified a crown-breakup mechanism, where Marangoni-driven holes are formed by splashing of a low-surface-tension liquid film. Finally, a rough count of holes in figure 4(f) shows that the crown breaks up by being punctured by a thousand holes.

REFERENCES

BREMOND, N. & VILLERMAUX, E. 2005 *J. Fluid Mech.* **524**, 121–130.

COSSALI, G. E., COGHE, A. & MARENGO, M. 1997 *Exps. Fluids* **22**, 463–472.

CULICK, F. E. C. 1960 *J. Appl. Phys.* **31**, 1128.

DANOV, K., IVANOV, I. B., ZAPRYANOV, Z. Z., NAKACHE, E. & RAHARIMALALA, S. 1988 In *Synergetics, Order and Chaos* (ed. M. G. Velarde), pp. 178–192. World Scientific.

DUSSAUD, A. D. & TROIAN, S. M. 1998 *Phys. Fluids* **10**, 23–38.

EDGERTON, H. E. & KILLIAN, J. R. 1939 *Flash! Seeing the Unseen by Ultra high-speed Photography*. Hale, Cushman & Flint, Boston.

ETOH, T. G., POGGEMANN, D., KREIDER, G. *et al.* 2003 *IEEE Trans. Electron Devices* **50**, 144–151.

GARETT, P. R. (ED.) 1993 *Defoaming, Theory and Industrial Applications*. Marcel Dekker.

JENSEN, O. E. 1995 *J. Fluid Mech.* **293**, 349–378.

RUCKENSTEIN, E., SMIGELSCHI, O. & SUCIU, D. G. 1970 *Chem. Engng Sci.* **25**, 1249–1254.

SANTIAGO-ROSANNE, M., VIGNES-ADLER, M. & VELARDE, M. G. 1997 *J. Colloid Interface Sci.* **191**, 65–80.

SONG, M. & TRYGGVASON, G. 1999 *Phys. Fluids* **11**, 2487–2493.

STERLING, C. V. & SCRIVEN, L. E. 1959 *AIChE J.* **5**, 514–523.

TAYLOR, G. I. 1959 *Proc. R. Soc. Lond.* A **253**, 313–321.

THORODDSEN, S. T. 2002 *J. Fluid Mech.* **451**, 373–381.

WANG, A.-B. & CHEN, C.-C. 2000 *Phys. Fluids* **12**, 2155–2158.

WORTHINGTON, A. M. 1908 *A Study of Splashes*. Longmans (Reprinted 1963, Macmillan).

XU, L., ZHANG, W. & NAGEL, S. R. 2005 *Phys. Rev. Lett.* **94**, 184505.

YARIN, A. L. & WEISS, D., A. 1995 *J. Fluid Mech.* **283**, 141–173.